

Investigation Into the Potential Value of Stratospheric Balloon Winds Assimilated in NOAA's Finite-Volume Cubed-Sphere Global Forecast System (FV3GFS)

Katherine E. Lukens^{1,2} , Kayo Ide³, and Kevin Garrett¹

¹NOAA/NESDIS/Center for Satellite Applications and Research (STAR), College Park, MD, USA, ²Cooperative Institute for Satellite Earth System Studies (CISESS), University of Maryland, College Park, MD, USA, ³University of Maryland, College Park, MD, USA

Key Points:

- Stratospheric winds observed by long-duration superpressure Loon balloons are assimilated in NOAA NWP, and the impact is assessed
- Loon wind assimilation leads to local improvements in short-term forecasts of the lower stratospheric circulation during the study period
- Loon wind assimilation significantly improves the tropical stratospheric response to the 2019 New Year sudden stratospheric warming event

Correspondence to:

K. E. Lukens,
katherine.lukens@noaa.gov

Citation:

Lukens, K. E., Ide, K., & Garrett, K. (2023). Investigation into the potential value of stratospheric balloon winds assimilated in NOAA's Finite-Volume Cubed-Sphere Global Forecast System (FV3GFS). *Journal of Geophysical Research: Atmospheres*, 128, e2022JD037526. <https://doi.org/10.1029/2022JD037526>

Received 19 JUL 2022
 Accepted 27 DEC 2022

Author Contributions:

Conceptualization: Kayo Ide, Kevin Garrett
Data curation: Katherine E. Lukens
Formal analysis: Katherine E. Lukens, Kayo Ide, Kevin Garrett
Funding acquisition: Kayo Ide, Kevin Garrett
Investigation: Katherine E. Lukens, Kayo Ide, Kevin Garrett
Methodology: Katherine E. Lukens, Kayo Ide, Kevin Garrett
Project Administration: Kayo Ide, Kevin Garrett
Resources: Katherine E. Lukens, Kayo Ide, Kevin Garrett
Supervision: Kayo Ide, Kevin Garrett
Validation: Katherine E. Lukens, Kayo Ide, Kevin Garrett
Visualization: Katherine E. Lukens, Kayo Ide, Kevin Garrett
Writing – original draft: Katherine E. Lukens

Abstract Near-space balloon networks have the potential to improve numerical weather prediction (NWP) through data assimilation (DA) by providing in situ observations in an otherwise data-sparse stratosphere. This study investigates the prospective value of stratospheric balloon winds to NOAA NWP by examining Loon data quality and conducting a 2-month observing system experiment (OSE) using NOAA's Finite-Volume Cubed-Sphere Global Forecast System. During the study period (December 2018–January 2019), Loon winds show good correspondence to collocated rawinsonde (RAOBS) winds, while a considerable difference in tropical stratospheric winds is observed between NOAA and ECMWF operational analyses. The OSE, one run with Loon winds assimilated and another without, suggests that additional stratospheric wind observations can improve NWP. Loon wind assimilation acts to decelerate the strong tropical easterly stratospheric jet west of where Loon winds are observed while accelerating less intense subtropical easterly motions. Differences in observation-minus-background statistics between the two runs reveal that the backgrounds for Loon winds and RAOBS winds and temperatures improve when Loon winds are assimilated. This positively impacts short-term forecasts of the lower stratospheric circulation during the study period. Additionally, Loon wind assimilation improves the tropical stratospheric response to the 2019 New Year sudden stratospheric warming (SSW) event by significantly reducing the short-term forecast error following the SSW. The findings emphasize the value of stratospheric winds toward improving global NWP, and imply the importance of including near-space observing systems in the Earth-observing architecture.

Plain Language Summary Networks of large superpressure balloons have the potential to address a known data gap in the global observing system by providing in situ observations of the lower stratosphere. This study investigates the potential value of stratospheric winds observed by Loon balloons to NOAA by conducting two experiments, one run with Loon winds added and another without, using NOAA's Finite-Volume Cubed-Sphere Global Forecast System over a 2-month period (December 2018–January 2019). Comparisons between the two runs reveal the impact of adding Loon winds to the system. We find that Loon winds act to weaken the strong tropical easterly stratospheric jet in the model near where Loon winds are observed. Differences between the observed and model background winds show that the addition of Loon winds helps to improve the model wind and temperature backgrounds in the stratosphere, leading to better short-term forecasts of the stratospheric circulation during the study period. Additionally, Loon winds help improve the prediction of changes to the tropical stratosphere brought on by the 2019 New Year sudden stratospheric warming event by significantly reducing the forecast error following the event. These results emphasize the benefit of adding in situ stratospheric wind observations to global forecast models.

1. Introduction

Long-duration stratospheric superpressure balloons have the potential to fill a known data gap in the current Earth-observing architecture. At present, stratospheric in situ observations of wind, temperature, and humidity are primarily gathered through the global radiosonde network; coverage extends into the stratosphere across Earth's continents but is quite limited over the oceans (see Durre et al., 2006, their fig. 1). Additional sources of observations that could reach the stratosphere are aerosol and trace gas sensors onboard commercial aircraft; however, spatial coverage is restricted to aircraft altitude and the extent of international flight paths (see Blot et al., 2021, their fig. 1). Satellites offer more expansive coverage of observations by remote sensing, for example,

Writing – review & editing: Katherine E. Lukens, Kayo Ide, Kevin Garrett

atmospheric motion vectors (AMVs) derived from tracking the motions of clouds and other moisture features, yet the coverage of these data sets rely on the presence of such features in the stratosphere which is atypical. Even the Aeolus satellite that observes winds in profile into the stratosphere using Doppler wind lidar is limited to single along-track line-of-sight wind observations (Reitebuch et al., 2009; Stoffelen et al., 2005). As such, filling the observation gap in the stratosphere may be of substantial benefit to data assimilation (DA) and numerical weather prediction (NWP) skill. Further, in situ stratospheric observations are critical for improving the depiction and prediction of upper atmospheric dynamics, the transport of mass and trace constituents, and the global circulation in NWP (Butchart, 2014; Wargan et al., 2018).

Over the years, superpressure balloon campaigns have been conducted to provide additional stratospheric observations for the purpose of aiding atmospheric and related research, including the Eole experiment (Hertzog et al., 2006; Morel & Bandeen, 1973), the Concordiasi campaign (Rabier et al., 2010), and the Loon project (Rhodes & Candido, 2021). Loon, a former subsidiary of Google's parent company Alphabet, launched over 1,000 large superpressure balloons during the years 2011–2021 to provide continuous connectivity to internet-deficient regions around the world for months at a time. The Loon balloon instrument payloads were leveraged for environmental observations, with a series of sensors onboard that downlinked information in near-real time, including 4-dimensional global positioning system (GPS) data, solar altitude relative to the balloon, and atmospheric observations.

The data acquired during Loon and other balloon campaigns have been exploited for a wide range of applications, including the validation of (re)analyses, evaluation of atmospheric gravity waves, and impact assessments in global DA (e.g., Conway et al., 2019; Corcos et al., 2021; Coy et al., 2019; Friedrich et al., 2017; Hertzog et al., 2004, 2008; Jewtoukoff et al., 2015; Lindgren et al., 2020; Nastrom, 1980; Plougonven et al., 2013; Podglajen et al., 2014; Schoeberl et al., 2017). Friedrich et al. (2017) investigated the use of Loon balloon data in verifying reanalysis fields. They concluded that winds from ECMWF Reanalysis (ERA)-Interim, Modern-Era Retrospective analysis for Research and Applications (MERRA), MERRA version 2 (MERRA-2), and Climate Forecast System version 2 (CFSv2) were all comparable with Loon winds in the Southern Hemisphere (SH) mid-latitudes, and that simulated trajectories from MERRA-2 most accurately represented the Loon trajectories. Conway et al. (2019) used Loon balloon observations to characterize the fluctuations in stratospheric wind speed caused by atmospheric waves to better understand the difference between modeled and observed balloon trajectories and improve modeled stratospheric transport. Schoeberl et al. (2017) derived and examined lower stratospheric gravity wave spectra from Loon observations and concluded that temperature amplitudes used to parameterize high-frequency gravity waves in models do not agree with what is observed, supporting the PreConcordiasi superpressure balloon analysis in Podglajen et al. (2016). Lindgren et al. (2020) presented a novel examination of the seasonality of stratospheric gravity wave amplitudes derived from 4 years of Loon observations. The study provided estimates of spectral slopes for different seasons and frequency windows toward improving gravity wave parameterizations in models. Coy et al. (2019) examined the impact of Loon wind assimilation on the NASA Goddard Earth Observing System (GEOS) during the 2014 SH winter. They found that Loon winds act to improve the 6-hr forecasts by reducing the zonal wind observation-minus-background (O-B) error by 1 m s^{-1} in the tropics and by 5 m s^{-1} in regions where the difference between the Loon winds and the control experiment analysis is large.

This study investigates the potential value of in situ Loon stratospheric wind observations to global NWP by conducting an observing system experiment (OSE) using NOAA's Finite-Volume Cubed-Sphere (Lin, 2004; Putman & Lin, 2007) Global Forecast System (FV3GFS). Results from this case study estimate the impact of additional stratospheric winds on the analysis and short-term forecast skill as well as the atmospheric response to the sudden stratospheric warming (SSW) event during the 2018–2019 boreal winter.

The structure of the article is as follows: Section 2 describes the Loon data quality and the potential to improve operational analysis winds in the tropical stratosphere. Section 3 describes the FV3GFS model and OSE setup. Section 4 discusses the OSE results. Section 5 summarizes the findings and conclusions.

2. Comparison of Observed and Operational Winds With Loon

Each Loon balloon configuration consisted of an instrument payload platform tethered to a tennis court-sized balloon specifically designed to withstand harsh stratospheric conditions. Atmospheric sensors onboard the

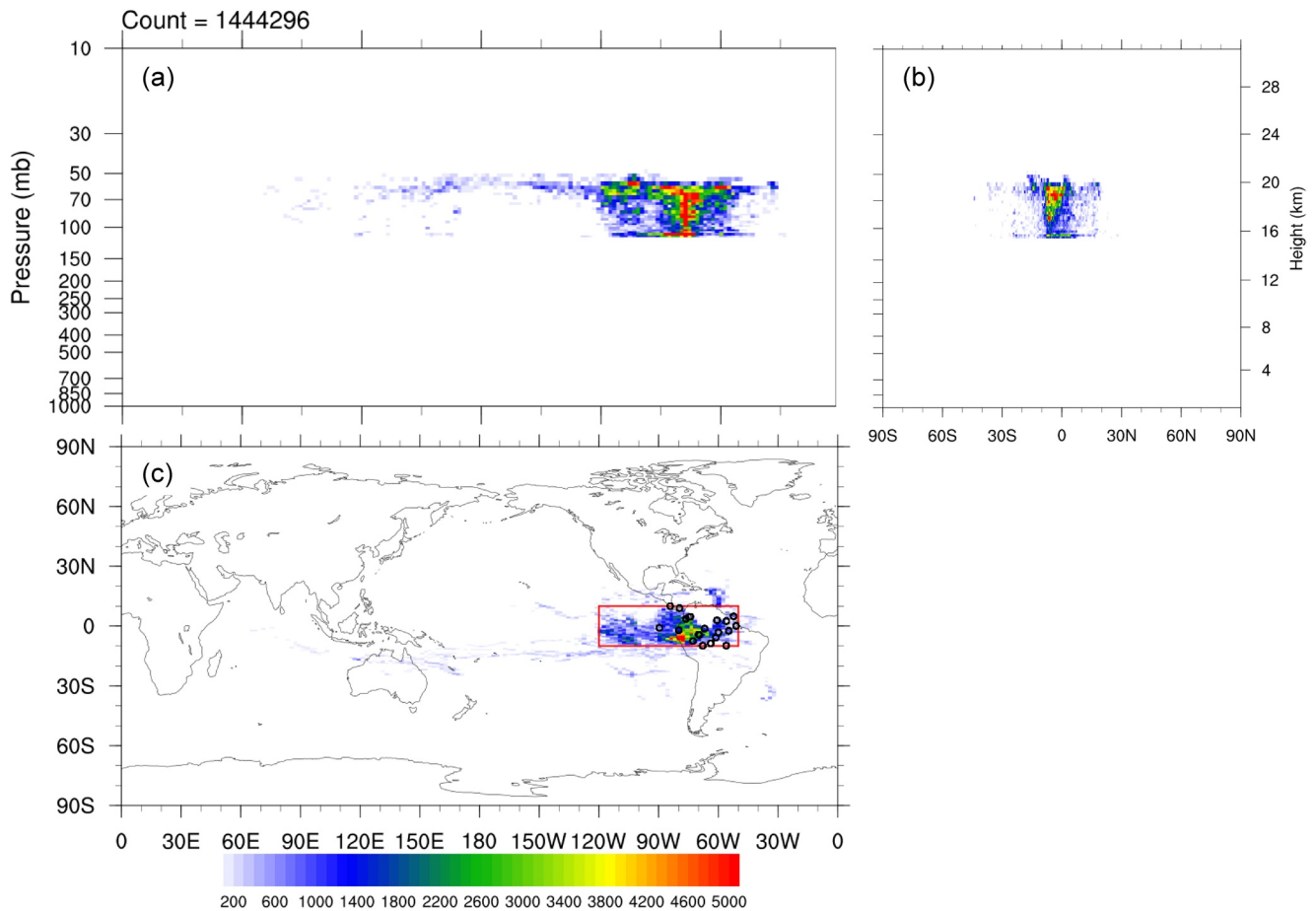


Figure 1. Density maps of assimilated Loon observations for the experiment period minus spin-up: 00 UTC December 8, 2018 –to 18 UTC January 31, 2019. Colors indicate total number of Loon observations within the cells plotted, which for (a, b) is 2.75 hPa per 1° latitude/longitude, and (c) 1° × 1°. The total number of observations shown is displayed above the upper left corner of panel (a). A red box outlines the Loon region (10°S–10°N and 120°–50°W). Black open circles denote the surface locations of the 19 rawinsonde stations within the Loon region.

platform observed the environment at balloon level in the lower stratosphere (~50–100 hPa) and were reported at a frequency of ~1 min. The data included geolocation (latitude, longitude, and geometric altitude) from the GPS onboard, pressure, temperature, and winds derived by a Kalman filter-smoothed estimate of backward-looking finite differences estimated from subsequent GPS positions along an individual trajectory. For additional details regarding the Loon dataset, see Rhodes and Candido (2021). Figure 1 displays the horizontal and vertical extent of the Loon observations available during the 2-month OSE period from 00 UTC December 8, 2018 through 18 UTC January 31, 2019. Note that the model spin-up period is December 1–7, 2018 and has been omitted from the assessment (see discussion in Section 3). The balloons were launched from the Caribbean and circumnavigated the globe following the eastward ambient flow until they reached the eastern equatorial Pacific Ocean/northern South America where they remained for several months. To keep the balloons aloft over the region, a ground team occasionally maneuvered the individual balloons by remotely adjusting the pressure of smaller balloons inside the larger ones to change the balloon altitude and hence catch different local airstreams. Because such intentional maneuvers can lead to large oscillations of the trajectories that potentially degrade the data quality, Loon winds required some preprocessing. The main preprocessing step was comprised of the identification and removal of data during the maneuver periods. Maneuvers were identified based on the authors' own calculations. An algorithm was devised to compute thresholds of incremental differences in pressure, height, and time between adjacent observations along each balloon trajectory, for example, the time difference threshold used was 250 s or two times the standard deviation. Maneuvers were identified and subsequently omitted when the thresholds for all three variables were exceeded at the same moment. The other main preprocessing step involved the removal of duplicate observations that were inherently included in the Loon data set. Duplicates were defined

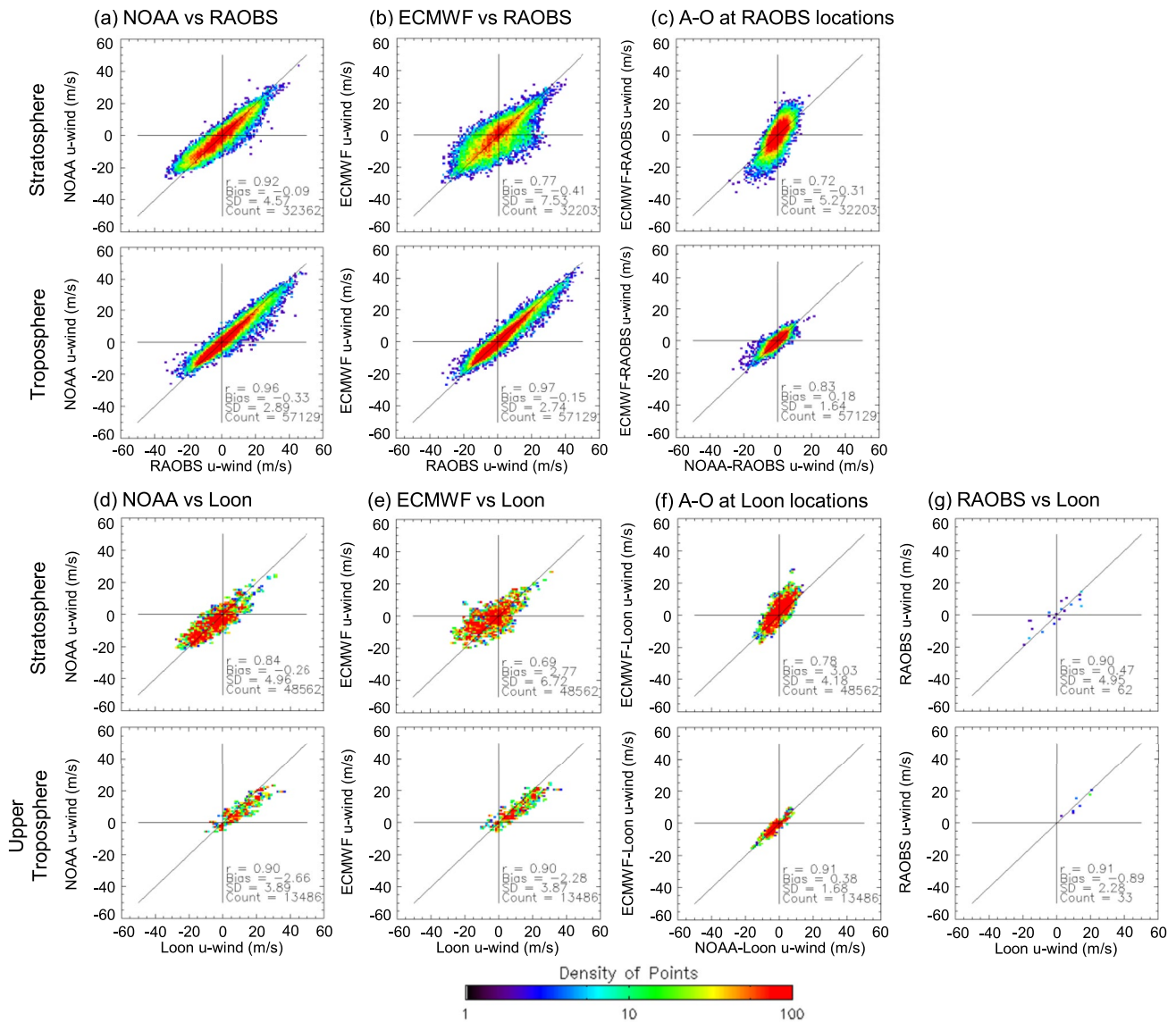


Figure 2. Density scatterplots of zonal wind (*u*-wind) comparisons over the eastern equatorial Pacific region at 00 UTC, covering the study period at rawinsonde (RAOBS) observation locations within the Loon region (10°S–10°N and 120°–50°W). Colors indicate the “density of points” or number of observation pairs within the plotted cells, which are 1 m s⁻¹ on a side. (a) NOAA GFS operational analysis versus RAOBS, (b) ECMWF operational analysis versus RAOBS, (c) the analysis minus observation (A-O) comparisons of ECMWF-RAOBS (*y*-axis) versus NOAA-RAOBS (*x*-axis). (d)–(f) As in (a)–(c) but versus Loon zonal wind at Loon locations within the Loon region. (g) RAOBS versus Loon. Note that the bottom panels of (d)–(g) characterize the upper troposphere, while the bottom panels in (a)–(c) characterize the entire troposphere. Mean sample statistics are displayed in the bottom right of each panel. Stratospheric and tropospheric comparisons are delineated by 100 hPa. Horizontal and vertical black lines indicate 0.0 m s⁻¹. Diagonal black line is the one-to-one line and indicates a perfect match. Units are m s⁻¹.

as observations with the same latitude/longitude coordinates as those immediately previous and adjacent along each balloon trajectory.

Figure 2 demonstrates large wind differences in current global NWP by way of density scatterplots for the study period comparing the 1° operational NOAA and ECMWF analysis zonal winds (or *u*-winds) with assimilated rawinsonde (RAOBS) *u*-winds in the stratosphere (in the first row) and troposphere (in the second row) in the Loon region (10°S–10°N and 120°–50°W, denoted by the red box in Figure 1c). The boundary between the stratosphere and troposphere is 100 hPa. (Note that the 1° ECMWF and NOAA operational winds were down-scaled from higher resolutions by the data producers, and the NOAA operational model used a spectral dynamical core until June 2019 (after the study period) when it was upgraded to the FV3 core.) Both operational data sets represented the global *u*-wind at the 00 UTC analysis time and were interpolated to the three-dimensional

RAOBS positions only for RAOBS with observation times within ± 1 hr of 00 UTC; note that since the ECMWF winds were only available at 00 UTC, only the NOAA winds at 00 UTC were included in Figure 2, for consistency. RAOBS station locations within the Loon region are plotted in Figure 1c for reference. RAOBS winds are dependent observations in that they are assimilated by both NOAA and ECMWF, and they use an observation error variance of $3^2 \text{ m}^2 \text{ s}^{-2}$. NOAA analysis u -winds and RAOBS u -winds are highly correlated throughout the vertical (0.92 in the stratosphere, 0.96 in the troposphere), with a mean bias of -0.3 m s^{-1} in the troposphere and a near-zero bias in the stratosphere (Figure 2a). The root-mean-square differences (RMSDs) are very similar to the standard deviations (SDs), and so the following discussions concerning SDs also apply to RMSDs. Uncertainty represented by SD in the stratosphere is 4.6 m s^{-1} and is larger than that in the troposphere (2.9 m s^{-1}).

ECMWF minus RAOBS comparisons (Figure 2b) in the troposphere yield a smaller mean bias (-0.15 m s^{-1}) and similar SD (2.7 m s^{-1}) to NOAA, but in the stratosphere they unexpectedly yield a much larger SD (7.5 m s^{-1}). The larger SD is mainly attributed to ECMWF considerably underestimating the observed tropical stratospheric u -wind during the experiment period (Figure 2b, top panel). This underestimation manifests as a non-Gaussian or nonnormal distribution in the collocated winds, highlighting the large differences between ECMWF and RAOBS in the tropical stratosphere, as opposed to the more normal distribution in Figure 2a attributable to smaller differences overall between NOAA and RAOBS winds (Figure 2a). The results imply that (a) a large difference exists between ECMWF and NOAA winds in the tropical stratosphere for December 2018 and January 2019, and (b) additional wind observations can potentially improve the operational analyses in this region.

The difference between the operational analysis winds in the stratosphere during the study period is made clear by comparing NWP analysis minus RAOBS winds (A-O) for NOAA and ECMWF (Figure 2c). Since O represents the observation against which the analysis A is compared, A-O is examined instead of O-A; in this way, NOAA and ECMWF versus observations can be easily understood, with each O at the origin. It should be noted that because the A-O differences contain both the bias in O and the bias in A, they cannot distinguish the amount of bias attributed to O or to A, only that some bias exists. The right column shows the density scatter plots of NOAA and ECMWF analyses with respect to each RAOBS observation. In the troposphere, NOAA and ECMWF u -winds show good correspondence as indicated by the A-O difference pairs generally falling along the one-to-one line that signifies a perfect match, with ECMWF A-O differences having a relatively small mean bias and SD (0.18 and 1.6 m s^{-1} , respectively) (Figure 2c, bottom panel). However, in the stratosphere, ECMWF winds are generally shown to be faster than NOAA at the same RAOBS locations, with ECMWF A-O differences exhibiting a bias twice as large (0.31 m s^{-1}) and an SD of 5.3 m s^{-1} that is over 300% higher than in the troposphere (Figure 2c, top panel). This confirms the difference between NOAA and ECMWF winds during the study period attributed to the underestimation in wind velocity by ECMWF in the tropical lower stratosphere, and suggests that an additional in situ observing system can help reduce the discrepancy between the operational analyses and improve the representation of winds across NWP systems.

To examine the quality of preprocessed Loon data as an additional observing system, the same plots as for RAOBS are shown in the third and fourth rows of Figure 2, with the fourth row showing upper tropospheric comparisons due to Loon's limited vertical extent into the troposphere. Loon winds are collocated with but not interpolated to RAOBS positions. The maximum horizontal and vertical distance allowed between collocated Loon and RAOBS winds are 100 km and $0.04 \log_{10}(\text{hPa})$, respectively. Although Loon comparisons exhibit larger biases in the upper troposphere (Figures 2d and 2e, bottom panels) relative to RAOBS (see Figures 2a and 2b, bottom panels), the comparisons are reasonable, as they show agreement between NOAA and ECMWF, supporting the relationship between the analysis winds and RAOBS. In the stratosphere during the study period, NOAA has a much smaller bias but higher SD relative to Loon u -winds (-0.26 and 5.0 m s^{-1} , respectively) (Figure 2d), while ECMWF minus Loon comparisons (Figure 2e) and A-O differences at Loon locations (Figure 2f) display underestimations in wind velocity similar to those shown in the RAOBS comparisons. Additionally, Loon and RAOBS winds closely match in space and time (Figure 2g) and show a similar mean absolute bias and uncertainty to NOAA in the stratosphere (see Figure 2d, top panel) and a smaller SD in the upper troposphere. For the case study presented here, Loon and NOAA winds more closely match in the stratosphere compared to ECMWF, with the latter noticeably disagreeing with collocated NOAA, Loon, and RAOBS winds. This is supported by a previous study that found that while both FV3GFS and ECMWF global winds exhibited large RMS errors in the stratosphere for May–July 2018, ECMWF errors were larger (Bentley, 2018). It should be noted that the lower 1° horizontal resolutions, temporal resolution, and few stratospheric levels available for the NWP analyses in our

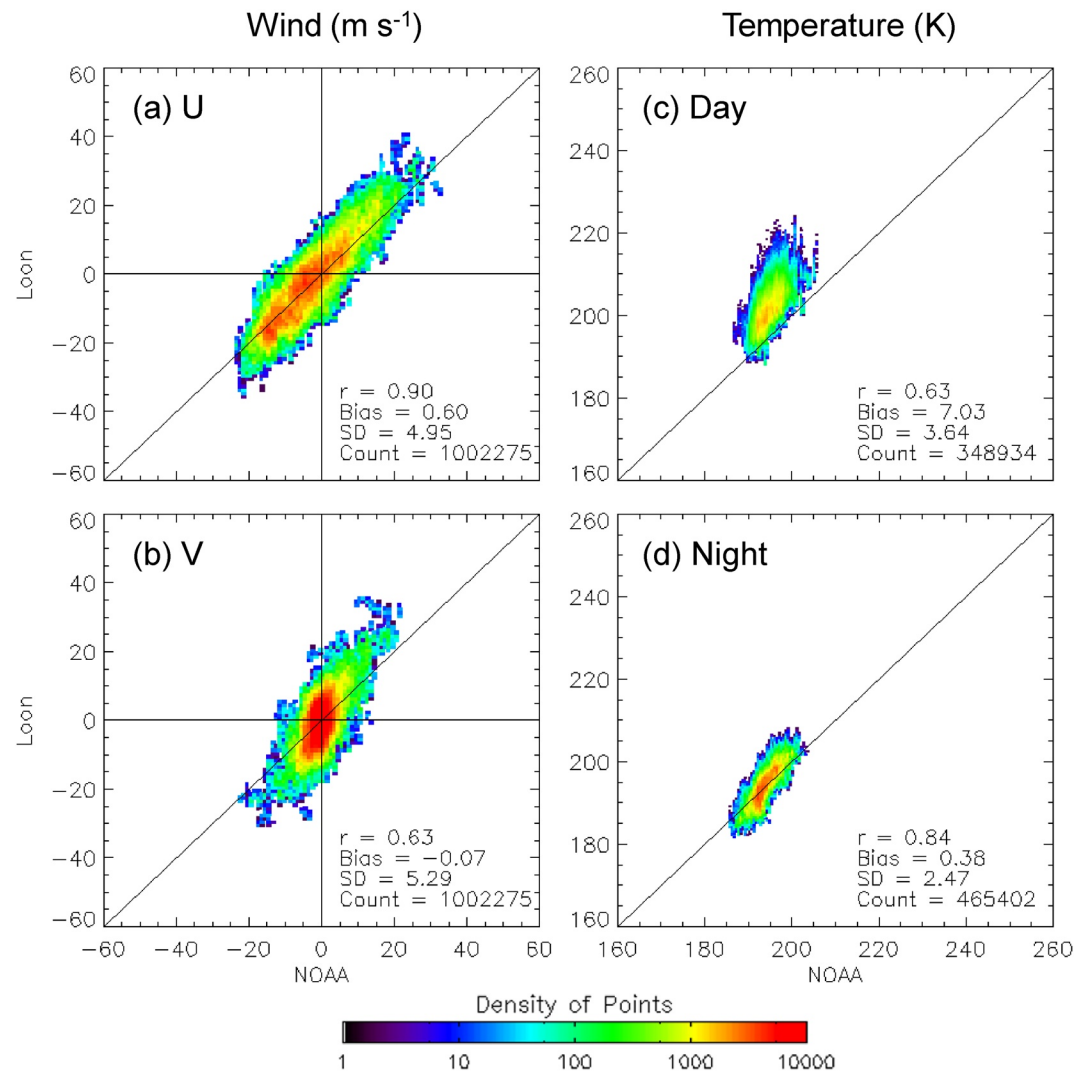


Figure 3. Density scatterplots of collocated Loon observations and NOAA GDAS at all four analysis times (00, 06, 12, and 18 UTC) over the study period. Columns are for (a)–(b) wind in m s^{-1} , and (c)–(d) temperature in K, with (a) zonal wind (u -wind), (b) meridional wind (v -wind), (c) temperature during local daytime, and (d) temperature during local nighttime. Colors indicate total number of collocated observation pairs within the cells plotted, which for (a, b) are 1 m s^{-1} , and (c, d) 0.5 K on a side. Mean sample statistics are displayed in the bottom right corner of each panel. Horizontal and vertical zero lines are plotted in black, as is the diagonal one-to-one line.

Figure 2 may contribute to the larger ECMWF minus NOAA differences by introducing sub-grid-related uncertainties in the stratosphere.

Differences in the operational stratospheric zonal wind analyses are also present in the meridional wind (or v -wind), although to a lesser degree (not shown). In the stratosphere, the NOAA v -wind exhibits a near-zero mean bias with an SD of 4.0 m s^{-1} that is comparable to the SD of NOAA u -wind relative to RAOBS (see Figure 2). As shown for u -wind, stratospheric ECMWF v -wind comparisons with RAOBS exhibit obvious underestimations in wind velocity with a larger mean bias (-0.28 m s^{-1}) and SD (5.0 m s^{-1}), suggesting that the NOAA and ECMWF v -winds also disagree in the stratosphere. In the troposphere, NOAA and ECMWF show good correspondence relative to RAOBS with similar SDs (2.8 – 2.9 m s^{-1}). Operational analysis v -wind versus Loon v -wind comparisons reveal similar relationships but with larger SDs (5 – 6 m s^{-1}).

In preparation for the OSE, preprocessed Loon winds as well as temperatures were compared to the 1° NCEP global analysis by NOAA's operational Global Data Assimilation System (GDAS) (Figure 3). The analysis data were interpolated to the 3D Loon locations for all Loon observations with observation times within $\pm 1 \text{ hr}$ of

the operational analysis time; unlike the comparisons in Figure 2, all available NOAA NWP analysis times (00, 06, 12, and 18 UTC) are included in the comparisons shown in Figure 3: this is the main difference between Figures 2d and 3a. Loon winds are generally in good agreement with NOAA. The u -wind distribution tends to follow the one-to-one line indicating a perfect match (Figure 3a). The mean bias is relatively small at 0.6 m s^{-1} and the uncertainty represented by SD is less than 5.0 m s^{-1} , in agreement with the results presented in Figure 2d. Similarly, the v -wind comparisons have a mean near-zero bias and an SD of 5.3 m s^{-1} (Figure 3b), despite Loon exhibiting larger magnitudes for faster winds. Although the difference between Loon and NOAA clearly exhibits some bias, the magnitude is much less than the difference between NOAA and ECMWF at Loon levels (see Figure 2), suggesting the potential impact to GDAS.

Loon and NOAA temperatures are compared during local daytime (Figure 3c) and nighttime (Figure 3d). Loon temperatures are largely overestimated in the daytime due to the direct exposure of the onboard wire temperature sensor to solar radiation, while at night in the absence of solar radiation Loon temperatures better correspond to NOAA ambient temperatures. Friedrich et al. (2017) investigated a way to remove the bias in temperature and concluded that such a bias correction is yet unable to sufficiently remove the effect of solar radiation for use in NWP. In line with this recommendation, and following the approach of Coy et al. (2019), the OSE presented here includes the assimilation of Loon winds only.

3. Model Description and OSE Setup

This study uses the NOAA FV3GFS, a hybrid four-dimensional ensemble variational (4D_{En}Var) system, with horizontal resolutions at C384 (25 km deterministic) and C192 (~50 km 80-member ensemble) and 64 vertical layers. Note that this DA system is different and newer than the NOAA operational product used to validate Loon winds in Section 2. The OSE includes two experiments: (a) a control experiment where Loon winds are monitored during the run but not assimilated, and (b) a second experiment with an identical setup to the control except that Loon winds are assimilated. The control is referred to as Loon_MON or \mathbf{x}_{MON} , and the assimilation experiment is referred to as Loon_ASM or \mathbf{x}_{ASM} . The OSE setup is similar to that in Coy et al. (2019) who employed a cubed-sphere grid in a 3DVar system to examine the impact of Loon winds in the SH on MERRA-2 DA.

The experiments each span a period of 2 months (00 UTC December 1, 2018 to 18 UTC January 31, 2019) using 18 UTC November 30, 2018 initial conditions. Fifty-five daily forecasts per forecast lead time (e.g., 24-hr and 96-hr) are included in the assessment for each deterministic run, with 55 equaling the total number of days in the experiment period minus the first 7 days (December 1–7, 2018) to account for model spin-up. Note that because the experiments cover a short time period, the results presented herein should only be considered as a case study.

As this is the first Loon assimilation study conducted using the FV3GFS, the experiments are set up with a simple observing system configuration. 1.4 million wind observations (per wind component) from 52 Loon balloons were assimilated as conventional data without bias correction, following the treatment of aircraft data in the FV3GFS, as a first step. To compensate for high temporal and spatial observations, observation error variance values assigned to all Loon winds were inflated to $10^2 \text{ m}^2 \text{ s}^{-2}$.

4. OSE Results

The forecast results are verified against their own self-analyses produced from the corresponding OSE runs at a 1° horizontal resolution. It should be noted that the variable relative humidity is not included in the following assessment, as the mean relative humidity (like wind) differs considerably between the NOAA and ECMWF analyses in the tropical lower stratosphere (not shown), which can overshadow the assessment results.

4.1. Overall Impact

Due to limited spatial coverage (see Figure 1), Loon wind assimilation has a localized influence on the analysis fields. Analysis increments show that the influence of Loon extends horizontally around the Loon locations by $\pm 5\text{--}10^\circ$ (~500–1,000 km) and vertically by $\pm 2\text{--}5$ km (not shown); these ranges of influence are similar to those presented in Coy et al. (2019). The extent of the influence is nearly equivalent to the GSI horizontal localization scale (~750–1,000 km at Loon levels) and vertical localization scale (0.5 log Pa), indicating that the spreading of the Loon observation influence is dictated by the DAS, as expected. The localized influence of

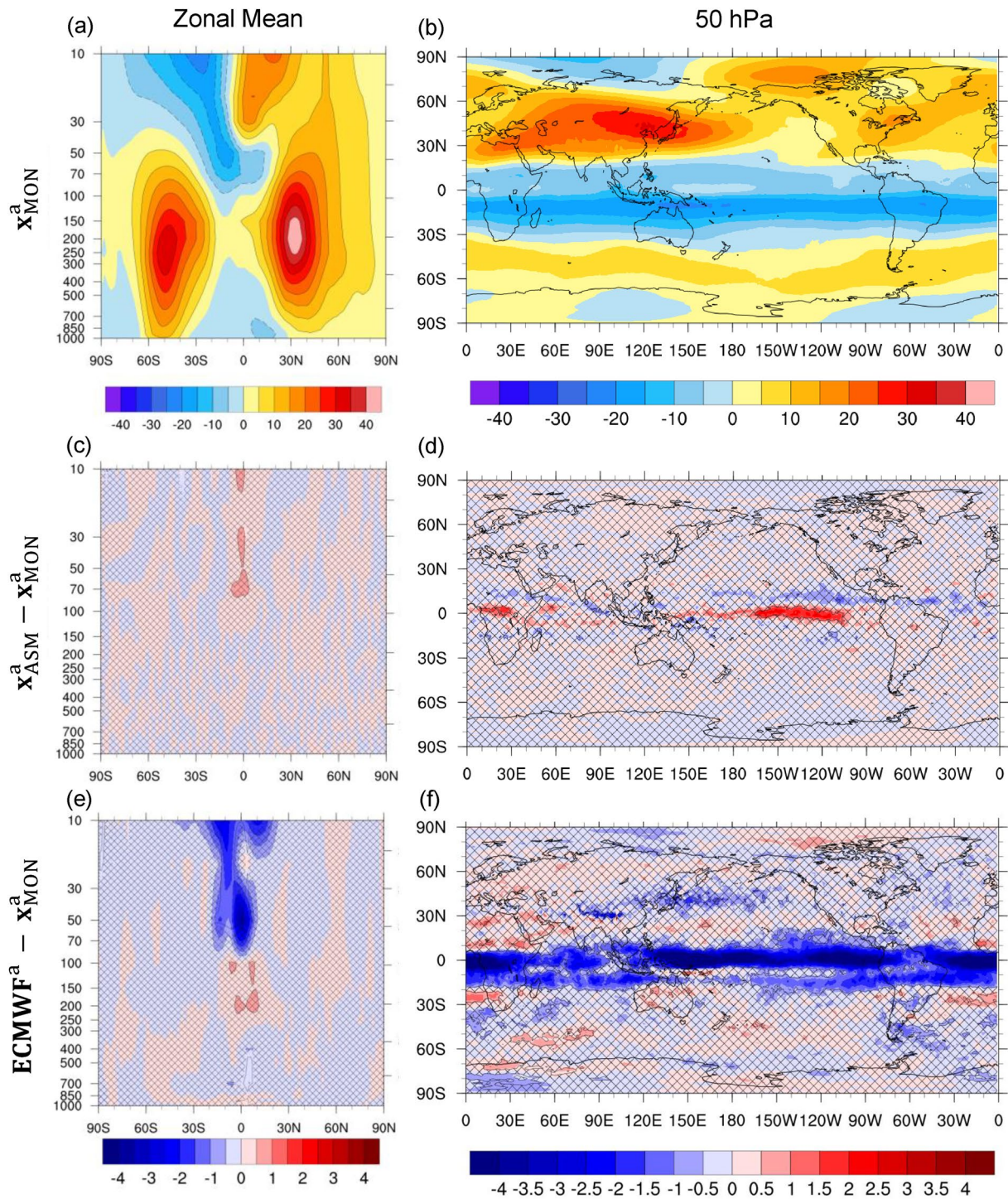


Figure 4. Mean analysis of zonal wind (u -wind) in m s^{-1} at 00 UTC, covering the study period. (Left column) Vertical zonal means, and (right column) mean horizontal cross-sections at 50 hPa. (a, b) x_{MON} , (c, d) x_{ASM} minus x_{MON} difference, and (e, f) ECMWF minus x_{MON} difference. Areas without hatching reveal statistically significant differences at the 95% level using the Student's t -test.

Loon wind assimilation on the analysis winds is clearly seen in the u -wind in Figure 4 by way of deviations of x_{ASM}^a (superscript a indicates the analysis) from x_{MON}^a in the tropical lower stratosphere. The x_{MON}^a u -wind distribution (Figures 4a and 4b) exhibits an easterly jet that persists throughout the tropics in the lower stratosphere. Loon wind assimilation leads to small wind differences within the easterly jet over the equatorial Pacific Ocean

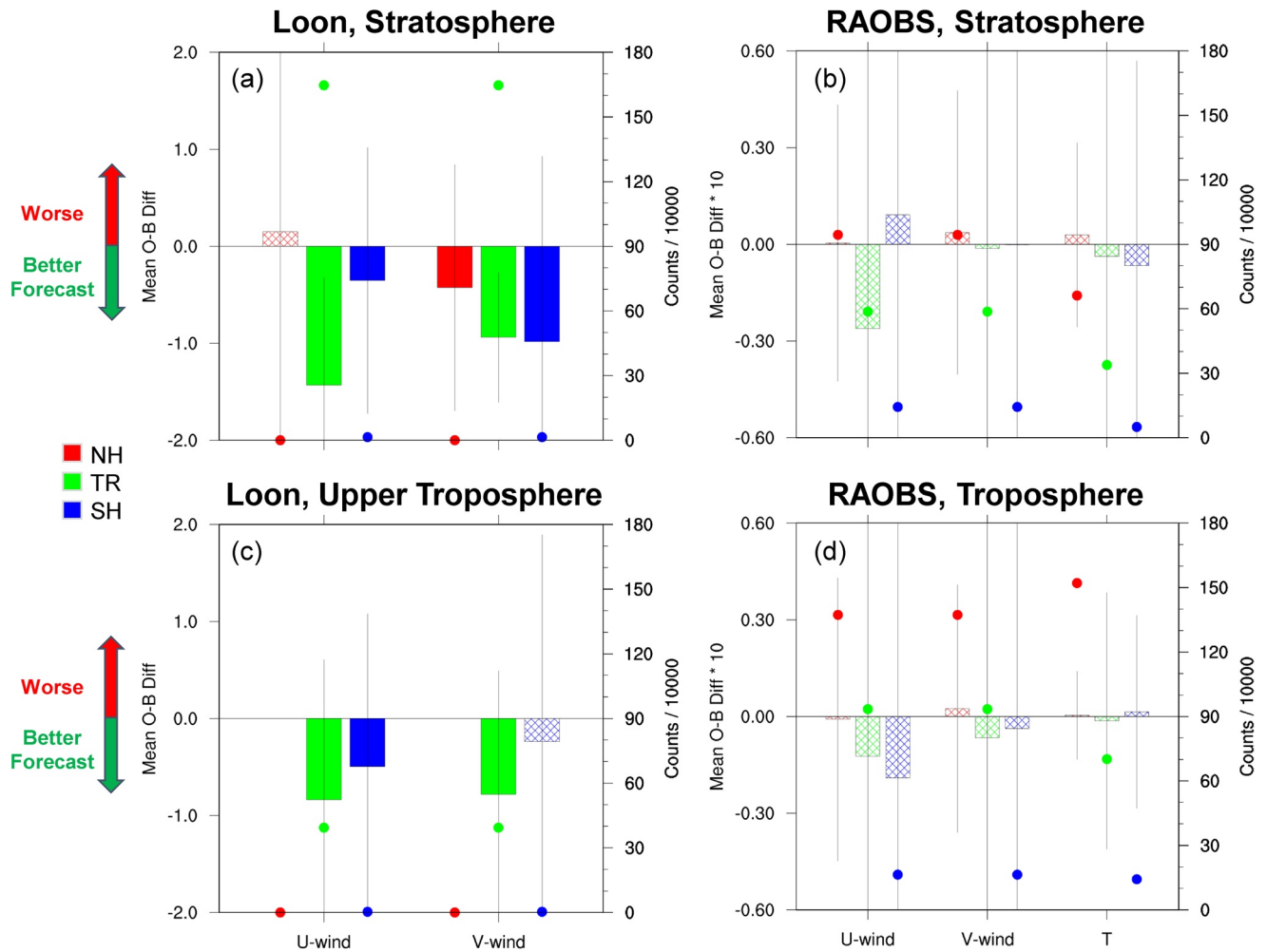


Figure 5. Mean differences in O-B for x_{ASM} minus x_{MON} in the NH (red), tropics (TR) (green), and SH (blue) separated by $\pm 30^\circ$ latitude in the stratosphere ($p < 100$ hPa) (top row) and troposphere ($p > 100$ hPa) (bottom row) for (a, c) Loon winds in $m s^{-1}$, and (b, d) RAOBS winds in $m s^{-1}$ and temperatures in K. Note that panel (c) characterizes the upper troposphere, while panel (d) characterizes the entire troposphere. Negative differences indicate the forecast has improved. Solid bars denote statistically significant differences at the 95% level, and hatched bars denote insignificant differences. Vertical lines attached to each bar show ± 1 standard deviation of the difference. Colored dots denote the observation count corresponding to each region.

west of where Loon observations are located (Figures 4c and 4d): statistically significant positive $x_{ASM}^a - x_{MON}^a$ differences (red colors) indicate a deceleration of the jet along the equator where it is stronger, and notable yet statistically insignificant negative differences (blue colors) around $\pm 15^\circ$ latitude indicate an acceleration of less intense easterly motions. Smaller, more localized differences are seen in the v -wind (not shown). In contrast, ECMWF analysis winds are significantly more easterly compared to x_{MON}^a winds (Figures 4e and 4f) and in turn to x_{ASM}^a winds (not shown) throughout the tropics. The relationships between Loon, NOAA, and ECMWF further emphasize the existence of a considerable difference between ECMWF and NOAA winds in the tropical stratosphere during the study period (see discussion in Section 2), and the potential of additional stratospheric winds toward improving NWP.

Figure 5 presents the effect of Loon wind assimilation on O-B statistics (Desroziers et al., 2005). Loon wind O-B statistics for x_{MON} are computed at Loon locations. Mean differences in Loon wind O-B between x_{ASM} and x_{MON} are negative and statistically significant in both the stratosphere ($p < 100$ hPa) (Figure 5a) and upper troposphere ($p > 100$ hPa) (Figure 5c), with the largest differences found in the tropics where the observation counts are highest. This result is expected and indicates that the background is improved for Loon winds where Loon winds are assimilated. Further, Loon wind assimilation has a notable albeit statistically insignificant positive effect on O-B statistics for RAOBS. For instance, u -wind O-B for RAOBS is largely reduced in the

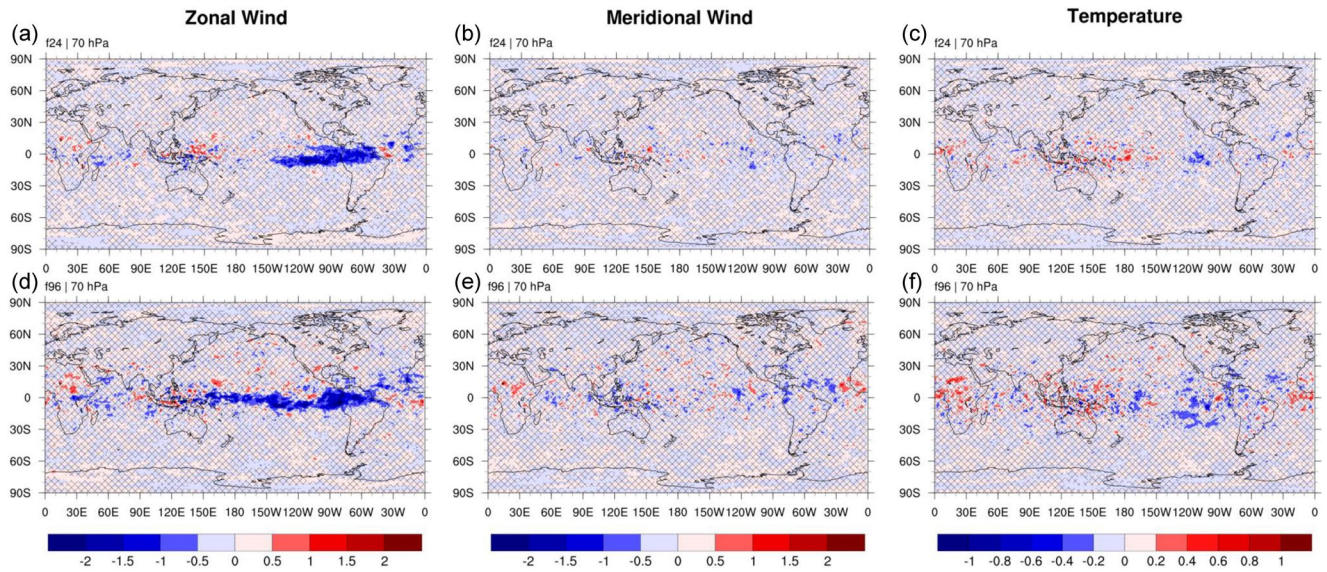


Figure 6. Δ RMSD for \mathbf{x}_{ASM}^f minus \mathbf{x}_{MON}^f at 70 hPa for 24-hr forecasts (top row), and 96-hr forecasts (bottom row): (a, d) Zonal wind (u -wind) in m s^{-1} , (b, e) meridional wind (v -wind) in m s^{-1} , and (c, f) temperature in K. Blue colors indicate the forecasts have improved. Areas without hatching reveal statistically significant differences at the 95% level using the Student's t -test.

tropical stratosphere (relative to other regions) (Figure 5b), suggesting that Loon wind assimilation leads to a local improvement in the background for RAOBS winds. RAOBS temperatures even show a small decrease in O-B in the stratosphere, further implying that Loon wind assimilation can help improve the background for other variables. In addition, Loon wind assimilation appears to have a small positive effect on both u -wind and v -wind O-B statistics for RAOBS throughout the troposphere where there are many more observations (Figure 5d), suggesting that Loon wind assimilation has an indirect positive effect on the background tropospheric circulation. A similar analysis was performed for aircraft observations and AMVs (not shown). O-B differences were quite small, with Loon having a mixed effect on aircraft winds and temperature, and a neutral impact on global AMVs.

To further demonstrate the potential of additional stratospheric winds, Figure 6 highlights the effect of Loon wind assimilation on forecast error in the lower stratosphere. Specifically, Figure 6 shows the difference in the RMSD (Δ RMSD) (Wilks, 2011) between \mathbf{x}_{ASM}^f and \mathbf{x}_{MON}^f (superscript f denotes the forecast) at two forecast lead times: 24-hr (day 1) and 96-hr (day 4). Equation (1) defines Δ RMSD:

$$\Delta\text{RMSD} = \text{RMSD}(\mathbf{x}_{ASM}^f, \mathbf{x}_v^a) - \text{RMSD}(\mathbf{x}_{MON}^f, \mathbf{x}_v^a) \quad (1)$$

where \mathbf{x}_{ASM}^f and \mathbf{x}_{MON}^f represent the forecasts from the assimilation and control experiments, respectively, and \mathbf{x}_v^a is the verification (self) analysis at the same time as the forecasts. If Δ RMSD < 0 (blue colors), Loon wind assimilation leads to a reduction in RMSD that signifies a positive impact. Hatches identify regions of statistical insignificance. At 70 hPa, Loon wind assimilation has a statistically significant positive impact on u -wind forecasts at latitudes where Loon observations are located (Figure 6a), supporting the finding that Loon wind assimilation has a localized influence on the forecasts. The significant positive impact on u -wind persists through day 4 and remains confined to the tropics (Figure 6d). By day 8 (not shown), the impact is global and mixed, with Δ RMSD no longer showing statistical significance, suggesting that the direct impact of Loon wind assimilation is limited to short-term forecasts (<5 days). Loon wind assimilation also results in a reduction—albeit much weaker than for u -wind—in the forecast RMSD for v -wind (Figures 6b and 6e) and temperature (Figures 6c and 6f) near where Loon observations are assimilated. The positive impact is confined to the tropics at day 1 and becomes stronger while spreading latitudinally with increasing lead time. The results indicate that Loon wind assimilation leads to improved forecasts of the lower stratospheric circulation, and this has greater implications for improving the prediction of the quasi-biennial oscillation and other stratospheric processes.

4.2. Response to an SSW Event

This study has the unique and fortunate opportunity to examine the potential importance of stratospheric wind observations toward improving the response to major SSW events. During a major event, planetary waves propagate into the stratosphere and break at high latitudes, inducing a slowdown of the polar stratospheric winds that prompts an enhanced mass flux toward the pole where air then descends and is heated adiabatically (Baldwin et al., 2021; Rao et al., 2019). This rapid increase in polar temperatures propagates down to the troposphere and is accompanied by an anomalous cooling of tropical stratospheric temperatures, with both phenomena persisting for several weeks following the SSW (Baldwin et al., 2021; Chandran & Collins, 2014). Sigmond et al. (2013) suggest that the tropospheric response to an SSW is easier to forecast compared to conditions before an SSW event. This implies the importance of additional stratospheric observations toward improving the global response to SSWs given that, for example, more accurate stratospheric conditions in forecast models have been shown to lead to an improved surface climate response to SSWs (Hardiman et al., 2012).

A widely used metric to identify major SSW events was recommended by Charlton and Polvani (2007) who adapted their algorithm from the World Meteorological Organization's (WMO) definition (WMO/IQSY, 1964): a major SSW has occurred when there is an increase in zonal mean temperature north of 60°N coupled with a change in sign of the zonal mean zonal wind from westerly to easterly at 60°N and 10 hPa. During the study period, the global circulation pattern in the experiments changed following the occurrence of a major SSW event during the 2019 New Year (Figure 7). In December 2018 before the SSW, lower stratospheric temperatures exhibited a similar spatial pattern to stratospheric zonal wind typically associated with an organized polar vortex (see Rao et al. (2019), their fig. 2). Right around the New Year, a pronounced positive stratospheric temperature anomaly (defined as a departure from the \bar{x}_{MON}^a time mean) developed at high latitudes (Figures 7c and 7d) concurrently with a change in sign of the high-latitude u -wind (Figures 7a and 7b), signifying a major SSW event, in agreement with the findings presented by Rao et al. (2019). At the same time, a negative stratospheric temperature anomaly was observed in the tropics (Figures 7e and 7f). In the following days to weeks, the large anomalies persisted and propagated down to the lower stratosphere/upper troposphere, and the Arctic polar vortex dynamically split and weakened (Butler et al., 2020; Lee & Butler, 2019; Rao et al., 2019, 2020). This resulted in the escape of very cold near-surface air out of the Arctic into lower latitudes, leading to a large mean decrease in near-surface temperatures over land at lower latitudes (e.g., as south as 30°N over North America).

Given that the global circulation changed following the 2019 New Year SSW, it is not surprising that the analysis and forecast skills for December 2018 and January 2019 differ (Figure 8). The forecast skills overall for \bar{x}_{MON} and \bar{x}_{ASM} in Figure 8 are captured by Summary Assessment Metrics (SAMs) (Hoffman et al., 2018) computed from weighted sums of normalized skill scores from NOAA's Verification Statistics DataBase (VSDB). The SAMs are stratified by forecast lead time, region, variable, and level, and each stratification includes skill scores from the other three parameters. Values above 0.5 indicate better performance and improved skill; by design, the sum of the two SAMs for each item is 1. Before the SSW (Figure 8a), Loon wind assimilation generally has a neutral impact on forecast skill for all parameters. After the SSW (Figure 8b), the skill is markedly improved, with the largest improvements appearing in the troposphere and SH (far from where Loon observations are located), and at later forecast lead times. Since Loon wind assimilation tends to have a more localized impact on the analysis and short-term forecasts (see Section 4.1), the larger improvements in skill likely stem from changes to the tropospheric circulation in response to the major SSW, as it has been suggested that tropospheric conditions are easier to forecast after the onset of an SSW event (Sigmond et al., 2013).

Figure 9 exhibits zonal mean forecast ΔRMSD over the course of the study period. The left column (Figures 9a–9g) shows the 24-hr forecast ΔRMSD for u -wind at 60°N, temperature north of 60°N, and temperature at the Equator, respectively, for a direct comparison with Figures 7a–7e. The ΔRMSD indicates that the impact of Loon wind assimilation is small, mixed, and confined to the tropics from a global mean perspective. However, the local impact of Loon wind assimilation becomes clear when the spatial scope is limited to the Loon region (as denoted by the red box in Figure 1c) (Figure 9 center and right columns): Loon wind assimilation leads to a notable reduction in u -wind and temperature RMSD in the tropical lower stratosphere from 24-hr (Figures 9b and 9h) to 96-hr (Figures 9c and 9i); a smaller reduction in v -wind RMSD is also observed (Figures 9e and 9f).

The contribution of Loon wind assimilation to the forecast skill of stratospheric conditions after the onset of an SSW event is presented in Figure 10. The left column highlights changes in the 24-hr forecast RMSD for the control experiment (\bar{x}_{MON}^f) in the lower stratosphere after the onset of the SSW, that is, ΔRMSD for January 2019

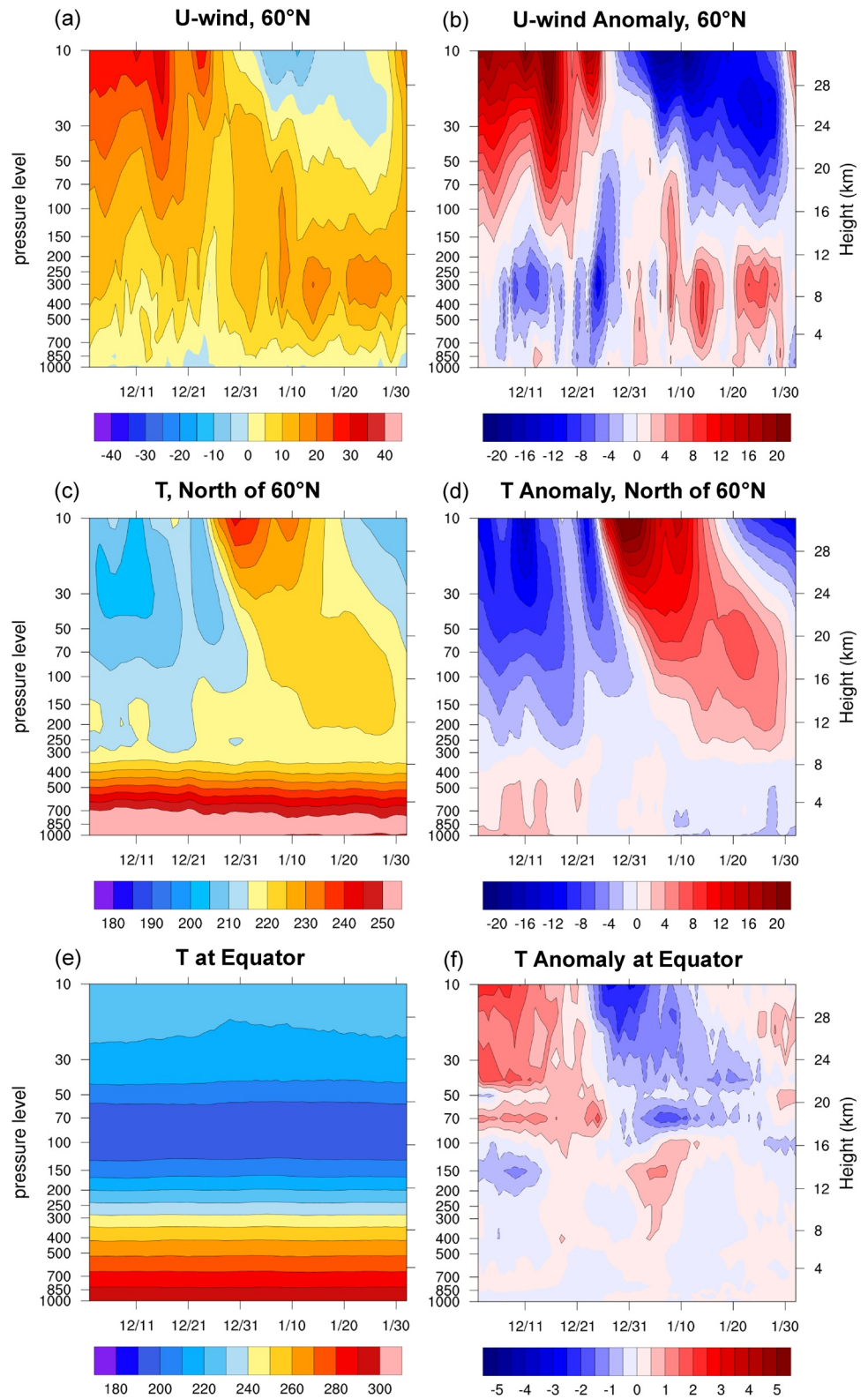


Figure 7. Zonal mean pressure-time sections of x_{MON}^a analysis fields (left column) and anomalies defined as departures from the x_{MON}^a time mean (right column) during the experiment period. (a, b) Zonal wind (u-wind) in m s^{-1} at 60°N, (c, d) mean temperature (T) in K north of 60°N, and (e, f) mean temperature in K at the Equator.

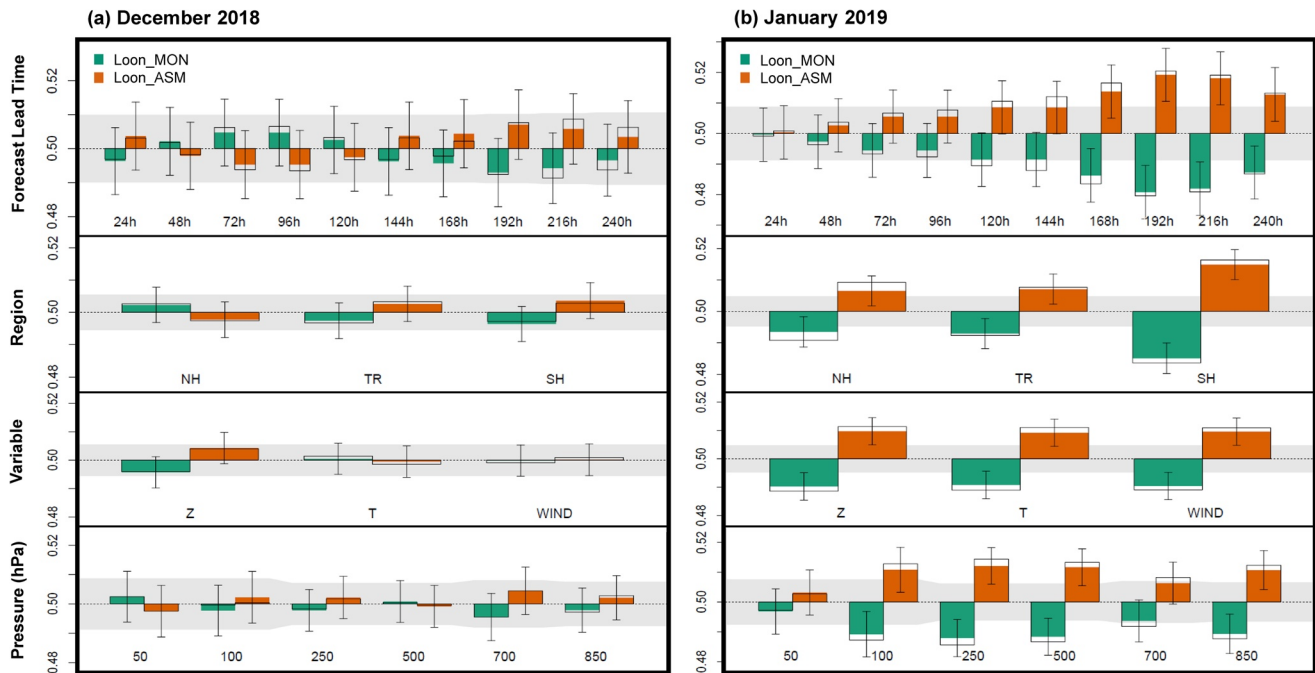


Figure 8. Summary Assessment Metrics (SAMs) comparing the control experiment (x_{MON}^f) in blue-green with the assimilation experiment (x_{ASM}^f) in red-orange, for December 8–31, 2018 (left) and January 1–31, 2019 (right). Each row shows normalized global statistics of the impact of assimilating stratospheric Loon winds on NOAA FV3GFS forecast skill with respect to: (top) forecast lead time; (upper-mid) geographic region including NH, TR, and SH; (lower-mid) variable including geopotential height (Z), temperature (T), and wind (includes u-wind and v-wind); and (bottom) pressure level in hPa. Values greater than 0.5 indicate positive impact. Shaded regions indicate the 95% confidence threshold. Error bars are attached to the ends of each colored bar.

minus December 2018 (Figures 10a, 10c, and 10e). For this case study, significant increases in u -wind and v -wind RMSD are coupled with significant RMSD reductions to the west over the tropical Pacific/Indian Oceans and the tropical Atlantic Ocean. Temperature RMSD exhibits a similar dipole pattern over Indonesia but shows an overall increase in the Western Hemisphere tropics (Figure 10e). The RMSD dipoles in the Eastern Hemisphere likely correspond to horizontal shifts in forecasted deep convection associated with the switch from Madden-Julian Oscillation (MJO) Phase 5 to MJO Phase 6 during the SSW event (Baldwin et al., 2021; Kodera, 2006; Rao et al., 2019). The right column in Figure 10 represents the impact of Loon wind assimilation on the 24-hr forecast skill during January 2019 after the SSW, that is, ΔRMSD for x_{ASM}^f minus x_{MON}^f (Figures 10b, 10d, and 10f). Loon wind assimilation has a statistically significant, positive impact on the 24-hr forecasts of winds and temperature near the Loon region over the eastern equatorial Pacific Ocean, where the x_{MON}^f RMSD increases after the SSW. Moreover, Loon wind assimilation is shown to further significantly reduce the RMSD in regions where the x_{MON}^f RMSD has already been reduced following the SSW, for example, over the central equatorial Pacific Ocean and northern South America for u -wind (Figure 10b). Similar results are found out to 96-hr in the lower stratosphere (not shown). The findings indicate that Loon wind assimilation helps to improve the short-term tropical stratospheric response to SSWs by balancing out any degradation that may occur in the forecasts while also further increasing the forecast skill in other regions.

5. Conclusions

Additional near-space observing systems are potentially of great value to the current Earth-observing architecture and global NWP. To explore the value of such systems to NOAA global NWP, a case study was conducted where in situ stratospheric winds observed by Loon superpressure balloons were assimilated in NOAA's FV3GFS. An OSE was performed that included two experiments: a control run and an identical experiment with Loon winds assimilated. Although the difference between Loon and NOAA winds exhibits some bias, the Loon data are assimilated without bias correction but with a higher observation error variance of $10^2 \text{ m}^2 \text{ s}^{-2}$ to account for the very large number of high-density observations (1.4 million per wind component) (Figure 1). The assimilation experiment results are compared against the control and verified against self-analyses. The experiments cover a period of 2 months (December 2018 to January 2019). The results presented here should only be considered as

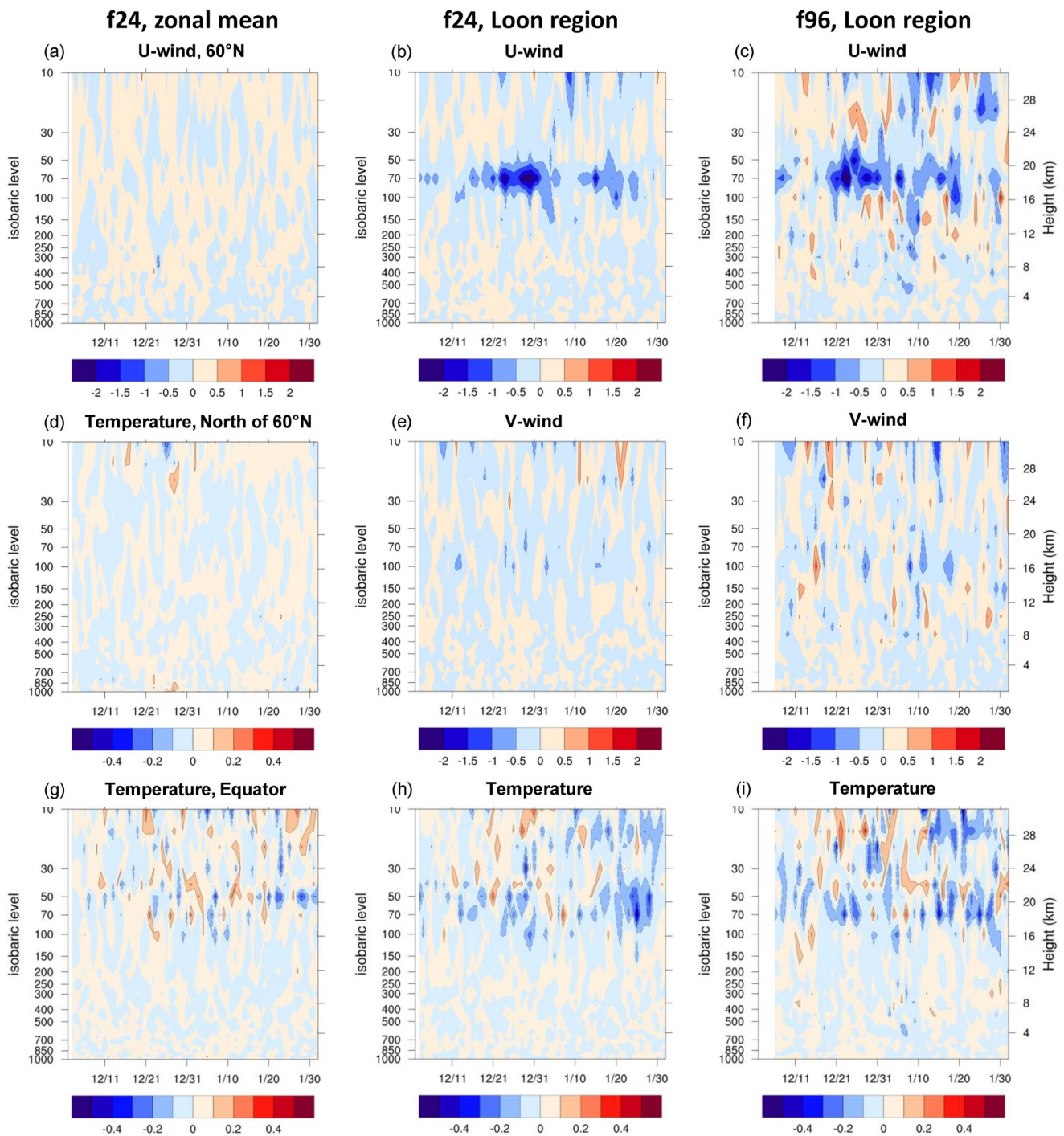


Figure 9. Pressure-time sections of differences in RMSD (Δ RMSD): Left column shows zonal mean 24-hr forecasts for (a) zonal wind (u-wind) in m s^{-1} at 60°N , (d) temperature in K north of 60°N , and (g) temperature in K at the Equator; center column shows 24-hr forecasts averaged over the Loon region (10°S – 10°N and 120° – 50°W) for (b) zonal wind in m s^{-1} , (e) meridional wind (v-wind) in m s^{-1} , and (h) temperature in K; (c, f, i) as in (b, e, h) but for 96-hr forecasts. Blue colors indicate the forecasts have improved.

a case study since the experiments cover a short time period, include a subset of Loon winds covering a small spatial domain, and use a simple observing system setup; specific impacts may vary when examining a different season or if Loon winds are distributed over a different region.

Because Loon balloons observe winds primarily in the tropical lower stratosphere, their inclusion in NWP could help reduce the large difference observed there in operational analysis winds during the study period. For this

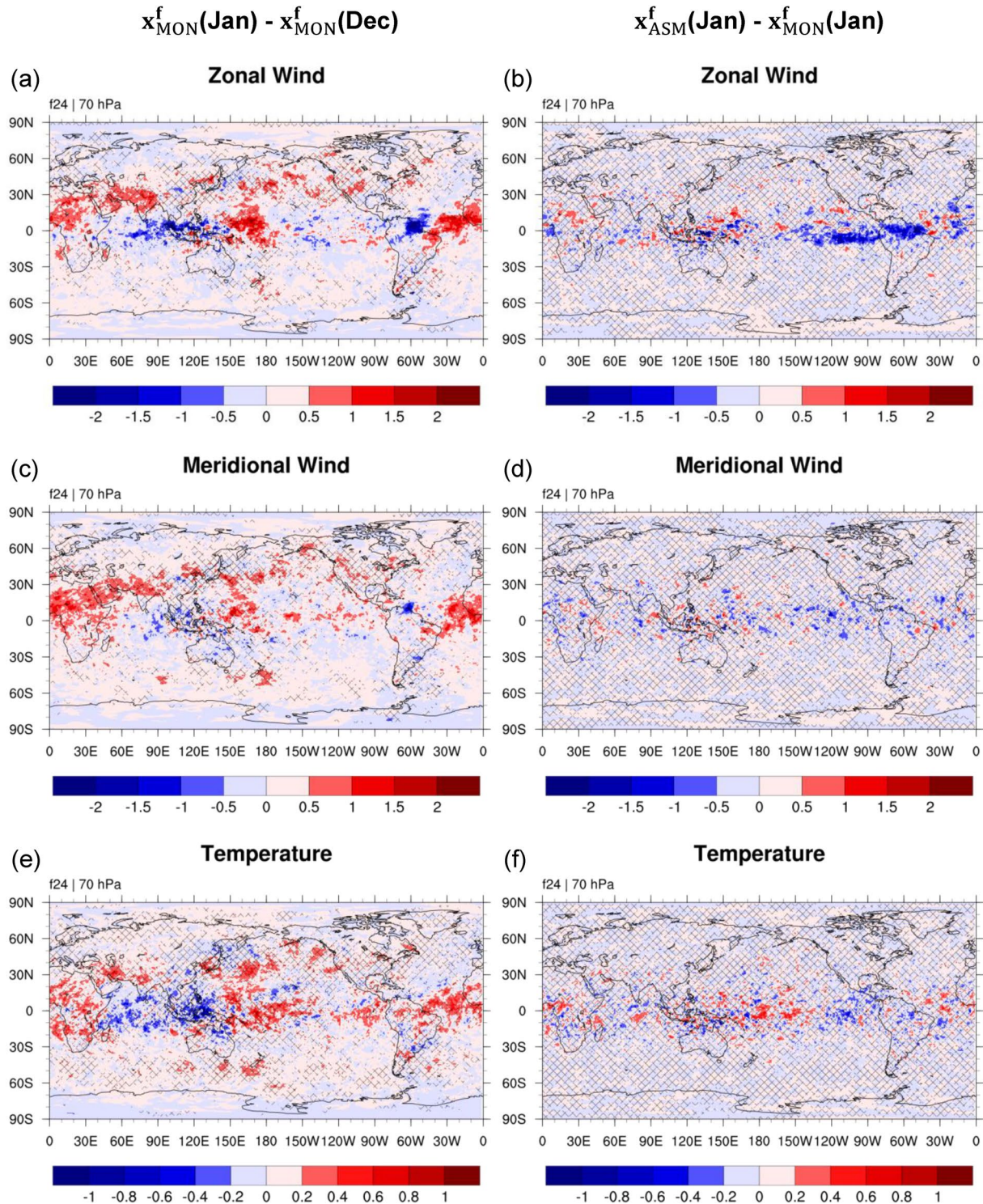


Figure 10. Differences in 24-hr forecast RMSD (Δ RMSD) at 70 hPa for (left column) x_{MON}^f between January 2019 minus December 2018, and (right column) January 2019 between x_{ASM}^f minus x_{MON}^f . (a, b) Zonal wind (u-wind) in $m s^{-1}$, (c, d) meridional wind (v-wind) in $m s^{-1}$, and (e, f) temperature in K. Areas without hatching reveal statistically significant differences at 95%. Blue colors indicate the forecasts have improved.

case study, Loon, NOAA, and ECMWF winds show good correspondence in the upper troposphere, and in the stratosphere Loon and NOAA match well (Figure 2), despite the difference between them exhibiting some bias (Figure 3). However, ECMWF winds in the stratosphere exhibit an unexpectedly larger SD that is attributed to ECMWF underestimating the observed wind velocity. In fact, NOAA and ECMWF easterly winds are signifi-

cantly different across the tropics in the stratosphere. Similar relationships are seen between the NWP analysis winds and Loon winds at Loon locations, with Loon-RAOBS comparisons yielding similar biases and uncertainties to NOAA-RAOBS comparisons. The results indicate that during the OSE period, NOAA and Loon winds more closely match in the tropical stratosphere compared to ECMWF, and additional wind observations have the potential to improve operational analyses in the region.

Loon wind assimilation has a local influence on the analysis fields. In the tropical lower stratosphere, Loon wind assimilation leads to a statistically significant deceleration of the strong easterly stratospheric jet over the equatorial Pacific Ocean west of where Loon winds are located (Figure 4). Differences in observation-minus-background statistics indicate that the background is significantly improved for Loon winds and notably but not significantly improved for RAOBS winds and temperatures in the tropics (Figure 5), implying that Loon wind assimilation leads to local improvements in the background stratospheric circulation. Moreover, Loon wind assimilation is shown to reduce the forecast RMSD in the tropical lower stratosphere out to 96-hr throughout the study period (Figures 6 and 9).

This study has the unique opportunity to examine the potential value of stratospheric wind observations toward improving the response to major SSW events. During the 2019 New Year, a major SSW event occurred that weakened the Arctic polar vortex and altered the global mean circulation (Figure 7). Before the SSW (December 2018), Loon wind assimilation is shown to have a generally neutral impact on global NWP, but after the SSW the forecast skill improved considerably (Figure 8). The largest improvements appear in the troposphere, SH, and at later forecast lead times, and are likely due to changes to the tropospheric circulation in response to the major SSW, as the forecast skill of tropospheric conditions is more likely to improve after an SSW event (Sigmond et al., 2013). Loon wind assimilation is shown to help improve the January 2019 forecast skill of tropical stratospheric conditions by reducing the forecast RMSD out to 96-hr (Figure 9), for example, over the eastern equatorial Pacific Ocean where the control forecasts degraded following the onset of the SSW event (Figure 10). In addition, Loon wind assimilation leads to a further decrease in the RMSD in regions where the control RMSD was reduced following the SSW. The results suggest that stratospheric wind observations can help significantly reduce short-term forecast error following an SSW.

The findings emphasize the value of in situ stratospheric wind observations toward improving global NWP, and imply the benefit of (a) including near-space observing systems like Loon in NWP and the Earth-observing architecture, and (b) increasing the vertical coverage of atmospheric winds and other observations to help close the stratospheric data gap. Future directions include the application of bias correction and improved quality controls for balloon data, as well as conducting OSEs over a longer time period.

Acknowledgments

The authors thank the Loon team, particularly Max Kamenetsky, James Antifaev, Sal Candido, Rob Carver, and Nikolai Chernyy, for willingly engaging in collaborations with NOAA and sharing their data and expertise in support of this project. The authors thank Chris Barnet, Hui Liu, Erin Jones, Likun Wang, and Ross N. Hoffman for their technical support and expertise that contributed to the analysis. Finally, the authors acknowledge Sid Boukabara for his leadership and support of the project. The University of Wisconsin-Madison S4 supercomputing system (Boukabara et al., 2016) was used in this work. The authors acknowledge support from the NOAA/NESDIS Office of Projects, Planning and Acquisition (OPPA) Technology Maturation Program (TMP) (NA14NES4320003 and NA19NES4320002) through CICS and CISESS at the University of Maryland/Earth System Science Interdisciplinary Center (ESSIC). The scientific results and conclusions, as well as any views or opinions expressed herein, are those of the authors and do not necessarily reflect those of NOAA or the U.S. Department of Commerce.

Conflict of Interest

The authors declare no conflicts of interest relevant to this study.

Data Availability Statement

The Loon balloon data used in this study are publicly available and can be accessed via the Zenodo open repository (<https://doi.org/10.5281/zenodo.3755988>) (Rhodes & Candido, 2021).

References

- Baldwin, M. P., Ayarzagüena, B., Birner, T., Butchart, N., Butler, A. H., Charlton-Perez, A. J., et al. (2021). Sudden stratospheric warmings. *Reviews of Geophysics*, 59, e2020RG000708. <https://doi.org/10.1029/2020RG000708>
- Bentley, A. (2018). *FV3GFS statistical update*. NCEP/EMC Model Evaluation Group. Retrieved from <https://www.emc.ncep.noaa.gov/users/meg/fv3gfs/>
- Blot, R., Nedelec, P., Boulanger, D., Wolff, P., Sauvage, B., Cousin, J.-M., et al. (2021). Internal consistency of the IAGOS ozone and carbon MONoxide measurements for the last 25 years. *Atmospheric Measurement Techniques*, 14, 3935–3951. <https://doi.org/10.5194/amt-14-3935-2021>
- Boukabara, S. A., Zhu, T., Tolman, H. L., Lord, S., Goodman, S., Atlas, R., et al. (2016). S4: An O2R/R2O infrastructure for optimizing satellite data utilization in NOAA numerical modeling systems, a step toward bridging the gap between research and operations. *Bulletin of the American Meteorological Society*, 97, 2359–2378. <https://doi.org/10.1175/bams-d-14-00188.1>
- Butchart, N. (2014). The Brewer-Dobson circulation. *Reviews of Geophysics*, 52, 157–184. <https://doi.org/10.1002/2013RG000448>

- Butler, A. H., Lawrence, Z. D., Lee, S. H., Lillo, S. P., & Long, C. S. (2020). Differences between the 2018 and 2019 stratospheric polar vortex split events. *Quarterly Journal of the Royal Meteorological Society*, *146*, 3503–3521. <https://doi.org/10.1002/qj.3858>
- Chandran, A., & Collins, R. L. (2014). Stratospheric sudden warming effects on winds and temperature in the middle atmosphere at middle and low latitudes: A study using WACCM. *Annales Geophysicae*, *32*, 859–874. <https://doi.org/10.5194/angeo-32-859-2014>
- Charlton, A. J., & Polvani, L. M. (2007). A new look at stratospheric sudden warmings. Part I: Climatology and modeling benchmarks. *Journal of Climate*, *20*(3), 449–469. <https://doi.org/10.1175/JCLI3996.1>
- Conway, J. P., Bodeker, G. E., Waugh, D. W., Murphy, D. J., Cameron, C., & Lewis, J. (2019). Using Project Loon superpressure balloon observations to investigate the inertial peak in the intrinsic wind spectrum in the midlatitude stratosphere. *Journal of Geophysical Research: Atmospheres*, *124*, 8594–8604. <https://doi.org/10.1029/2018JD030195>
- Corcos, M., Hertzog, A., Plougonven, R., & Podglajen, A. (2021). Observation of gravity waves at the tropical tropopause using superpressure balloons. *Journal of Geophysical Research: Atmospheres*, *126*, e2021JD035165. <https://doi.org/10.1029/2021JD035165>
- Coy, L., Schoeberl, M. R., Pawson, S., Candido, S., & Carver, R. W. (2019). Global assimilation of Loon stratospheric balloon observations. *Journal of Geophysical Research: Atmospheres*, *124*, 3005–3019. <https://doi.org/10.1029/2018JD029673>
- Desroziers, G., Berre, L., Chapnik, B., & Poli, P. (2005). Diagnosis of observation, background and analysis-error statistics in observation space. *Quarterly Journal of the Royal Meteorological Society*, *131*, 3385–3396. <https://doi.org/10.1256/qj.05.108>
- Durre, I., Vose, R. S., & Wuertz, D. B. (2006). Overview of the integrated global radiosonde archive. *Journal of Climate*, *19*, 53–68. <https://doi.org/10.1175/JCLI3594.1>
- Friedrich, L. S., McDonald, A. J., Bodeker, G. E., Cooper, K. E., Lewis, J., & Paterson, A. J. (2017). A comparison of Loon balloon observations and stratospheric reanalysis products. *Atmospheric Chemistry and Physics*, *17*, 855–866. <https://doi.org/10.5194/acp-17-855-2017>
- Hardiman, S. C., Butchart, N., Hinton, T. J., Osprey, S. M., & Gray, L. J. (2012). The effect of a well-resolved stratosphere on surface climate: Differences between CMIP5 simulations with high and low top versions of the Met Office climate model. *Journal of Climate*, *25*, 7083–7099. <https://doi.org/10.1175/JCLI-D-11-00579.1>
- Hertzog, A., Basdevant, C., & Vial, F. (2006). An assessment of ECMWF and NCEP-NCAR Reanalyses in the Southern Hemisphere at the end of the presatellite era: Results from the EOLE experiment (1971–72). *Monthly Weather Review*, *134*, 3367–3383. <https://doi.org/10.1175/MWR3256.1>
- Hertzog, A., Basdevant, C., Vial, F., & Mechoso, C. R. (2004). The accuracy of stratospheric analyses in the northern hemisphere inferred from long-duration balloon flights. *Quarterly Journal of the Royal Meteorological Society*, *130*, 607–626. <https://doi.org/10.1256/qj.03.76>
- Hertzog, A., Boccarra, G., Vincent, R. A., Vial, F., & Cocquerez, P. (2008). Estimation of gravity wave momentum flux and phase speeds from quasi-Lagrangian stratospheric balloon flights. Part II: Results from the Vorcore c0a campaign in Antarctica. *Journal of the Atmospheric Sciences*, *65*, 3056–3070. <https://doi.org/10.1175/2008JAS2710.1>
- Hoffman, R. N., Kumar, V. K., Boukabara, S.-A., Ide, K., Yang, F., & Atlas, R. (2018). Progress in forecast skill at three leading global operational NWP centers during 2015–17 as seen in Summary Assessment Metrics (SAMs). *Weather and Forecasting*, *33*, 1661–1679. <https://doi.org/10.1175/WAF-D-18-0117.1>
- Jewtoukoff, V., Hertzog, A., Plougonven, R., Cámara, A. d. l., & Lott, F. (2015). Comparison of gravity waves in the Southern Hemisphere derived from balloon observations and the ECMWF analyses. *Journal of the Atmospheric Sciences*, *72*(9), 3449–3468. <https://doi.org/10.1175/JAS-D-14-0324.1>
- Kodera, K. (2006). Influence of stratospheric sudden warming on the equatorial troposphere. *Geophysical Research Letters*, *33*, L06804. <https://doi.org/10.1029/2005GL024510>
- Lee, S. H., & Butler, A. H. (2019). The 2018–2019 Arctic stratospheric polar vortex. *Weather*, *75*, 52–57. <https://doi.org/10.1002/wea.3643>
- Lin, S.-J., (2004). A “vertically Lagrangian” finite-volume dynamical core for global models. *Monthly Weather Review*, *132*, 2293–2307. [https://doi.org/10.1175/1520-0493\(2004\)132<2293:AVLFDG>2.0.CO;2](https://doi.org/10.1175/1520-0493(2004)132<2293:AVLFDG>2.0.CO;2)
- Lindgren, E. A., Sheshadri, A., Podglajen, A., & Carver, R. W. (2020). Seasonal and latitudinal variability of the gravity wave spectrum in the lower stratosphere. *Journal of Geophysical Research: Atmospheres*, *125*, e2020JD032850. <https://doi.org/10.1029/2020JD032850>
- Morel, P., & Bandeen, W. (1973). The Eole experiment: Early results and current objectives. *Bulletin of the American Meteorological Society*, *54*, 298–306. <https://doi.org/10.1175/1520-0477-54.4.298>
- Nastrom, G. D. (1980). The response of superpressure balloons to gravity waves. *Journal of Applied Meteorology*, *19*, 1013–1019. [https://doi.org/10.1175/1520-0450\(1980\)019<1013:TROSBT>2.0.CO;2](https://doi.org/10.1175/1520-0450(1980)019<1013:TROSBT>2.0.CO;2)
- Plougonven, R., Hertzog, A., & Guez, L. (2013). Gravity waves over Antarctica and the Southern Ocean: Consistent momentum fluxes in mesoscale simulations and stratospheric balloon observations. *Quarterly Journal of the Royal Meteorological Society*, *139*, 101–118. <https://doi.org/10.1002/qj.1965>
- Podglajen, A., Hertzog, A., Plougonven, R., & Legras, B. (2016). Lagrangian temperature and vertical velocity fluctuations due to gravity waves in the lower stratosphere. *Geophysical Research Letters*, *43*, 3543–3553. <https://doi.org/10.1002/2016GL068148>
- Podglajen, A., Hertzog, A., Plougonven, R., & Žagar, N. (2014). Assessment of the accuracy of (re)analyses in the equatorial lower stratosphere. *Journal of Geophysical Research: Atmospheres*, *119*, 11166–11188. <https://doi.org/10.1002/2014JD021849>
- Putman, W. M., & Lin, S.-J., (2007). Finite-volume transport on various cubed-sphere grids. *Journal of Computational Physics*, *227*, 55–78. <https://doi.org/10.1016/j.jcp.2007.07.022>
- Rabier, F., Bouchard, A., Brun, E., Doerenbecher, A., Guedj, S., Guidard, V., et al. (2010). The CONCORDIASI project in Antarctica. *Bulletin of the American Meteorological Society*, *91*(1), 69–86. <https://doi.org/10.1175/2009BAMS2764.1>
- Rao, J., Garfinkel, C. I., Chen, H., & White, I. P. (2019). The 2019 New Year stratospheric sudden warming and its real-time predictions in multiple S2S models. *Journal of Geophysical Research: Atmospheres*, *124*, 11155–11174. <https://doi.org/10.1029/2019JD030826>
- Rao, J., Garfinkel, C. I., & White, I. P. (2020). Predicting the downward and surface influence of the February 2018 and January 2019 sudden stratospheric warming events in subseasonal to seasonal (S2S) models. *Journal of Geophysical Research: Atmospheres*, *125*, e2019JD031919. <https://doi.org/10.1029/2019JD031919>
- Reitebuch, O., Lemmerz, C., Nagel, E., Paffrath, U., Durand, Y., Endemann, M., et al. (2009). The airborne demonstrator for the direct-detection Doppler wind lidar ALADIN on ADM-Aeolus. Part I: Instrument design and comparison to satellite instrument. *Journal of Atmospheric and Oceanic Technology*, *26*, 2501–2515. <https://doi.org/10.1175/2009JTECHA1309.1>
- Rhodes, B., & Candido, S. (2021). Loon stratospheric sensor data [Dataset]. Zenodo. <https://doi.org/10.5281/zenodo.3755988>
- Schoeberl, M. R., Jensen, E., Podglajen, A., Coy, L., Lodha, C., Candido, S., & Carver, R. (2017). Gravity wave spectra in the lower stratosphere diagnosed from project loon balloon trajectories. *Journal of Geophysical Research: Atmospheres*, *122*, 8517–8524. <https://doi.org/10.1002/2017JD026471>
- Sigmond, M., Scinocca, J. F., Kharin, V. V., & Shepard, T. G. (2013). Enhanced seasonal forecast skill following stratospheric sudden warmings. *Nature Geoscience*, *6*(2), 98–102. <https://doi.org/10.1038/NNGEO1698>

- Stoffelen, A., Pailleux, J., Källén, E., Vaughan, J. M., Isaksen, L., Flamant, P., et al. (2005). The atmospheric dynamics mission for global wind field measurement. *Bulletin of the American Meteorological Society*, 86, 73–87. <https://doi.org/10.1175/BAMS-86-1-73>
- Wargan, K., Orbe, C., Pawson, S., Ziemke, J. R., Oman, L. D., Olsen, M. A., et al. (2018). Recent decline in extratropical lower stratospheric ozone attributed to circulation changes. *Geophysical Research Letters*, 45, 5166–5176. <https://doi.org/10.1029/2018GL077406>
- Wilks, D. (2011). *Statistical methods in the atmospheric sciences* (Vol. 100, 3rd ed.). Academic Press.
- World Meteorological Organization (WMO). (1964). *International years of the Quiet Sun (IQSY)*. Alert messages with special references to stratwarms. WMO/IQSY Report No 6, Secretariat of the World Meteorological Organization. World Meteorological Organization. Retrieved from https://library.wmo.int/doc_num.php?explnum_id=6525/